

Horizontal chromosome transfer and independent evolution drive diversification in *Fusarium oxysporum* f. sp. *fragariae*

Peter M. Henry¹ , Dominique D.A. Pincot² , Bradley N. Jenner³, Celia Borrero⁴ , Manuel Aviles⁴, Myeong-Hyeon Nam⁵, Lynn Epstein³ , Steven J. Knapp²  and Thomas R. Gordon³

¹United States Department of Agriculture, Agricultural Research Service, 1636 E. Alisal St., Salinas, CA 93905, USA; ²Department of Plant Sciences, University of California, One Shields Avenue, Davis, CA 95616, USA; ³Department of Plant Pathology, University of California, One Shields Avenue, Davis, CA 95616, USA; ⁴Department of Ciencias Agroforestales, Escuela Técnica Superior de Ingeniería Agronómica, Universidad de Sevilla, Ctra. Utrera km 1, Sevilla 41013, Spain; ⁵Strawberry Research Institute, Chungcheongnam-do Agricultural Research & Extension Services, Nonsan 32914, Korea

Author for correspondence:
Peter M. Henry
Email: peter.henry@usda.gov

Received: 4 June 2020
Accepted: 2 December 2020

New Phytologist (2021)
doi: 10.1111/nph.17141

Key words: convergent evolution, *Fragaria* × *ananassa*, *Fusarium* wilt, horizontal chromosome transfer, pathogen resistance, strawberry.

Summary

- The genes required for host-specific pathogenicity in *Fusarium oxysporum* can be acquired through horizontal chromosome transfer (HCT). However, it is unknown if HCT commonly contributes to the diversification of pathotypes.
- Using comparative genomics and pathogenicity phenotyping, we explored the role of HCT in the evolution of *F. oxysporum* f. sp. *fragariae*, the cause of *Fusarium* wilt of strawberry, with isolates from four continents.
- We observed two distinct syndromes: one included chlorosis ('yellows-*fragariae*') and the other did not ('wilt-*fragariae*'). All yellows-*fragariae* isolates carried a predicted pathogenicity chromosome, 'chr^{Y-frag}', that was horizontally transferred at least four times. chr^{Y-frag} was associated with virulence on specific cultivars and encoded predicted effectors that were highly upregulated during infection. chr^{Y-frag} was not present in wilt-*fragariae*; isolates causing this syndrome evolved pathogenicity independently. All origins of *F. oxysporum* f. sp. *fragariae* occurred outside of the host's native range.
- Our data support the conclusion that HCT is widespread in *F. oxysporum*, but pathogenicity can also evolve independently. The absence of chr^{Y-frag} in wilt-*fragariae* suggests that multiple, distinct pathogenicity chromosomes can confer the same host specificity. The wild progenitors of cultivated strawberry (*Fragaria* × *ananassa*) did not co-evolve with this pathogen, yet we discovered several sources of genetic resistance.

Introduction

Fusarium oxysporum is a species complex containing many host-specific pathogenic forms (called *formae speciales*). Pathogenic strains of *F. oxysporum* cause devastating crop losses worldwide, but most *formae speciales* have poorly characterised evolutionary origins. This includes *F. oxysporum* f. sp. *fragariae* (Fof), which causes *Fusarium* wilt of strawberry (strawberry = *Fragaria* × *ananassa* Duchesne ex Rozier). This pathogen was first reported in eastern Australia in 1962 and soon thereafter in Japan (1969) and South Korea (1974) (Winks & Williams, 1965; Okamoto *et al.*, 1970; Kim *et al.*, 1982). New reports of this disease surged globally during the early 2000s, including in major fruit production regions in California (2006) and Spain (2014) (Borrero *et al.*, 2017; Henry *et al.*, 2017). The evolutionary processes leading to the emergence of Fof remain uncharacterised, and it is unknown if the expanding geographic range of this pathogen resulted from dispersal or independent evolution of pathogenicity.

Although the exchange of DNA through meiotic recombination has never been documented for *F. oxysporum* (Taylor *et al.*, 2015), genetic exchange can occur via horizontal chromosome transfer (HCT), a process involving the transfer of 'accessory' chromosomes (Ma *et al.*, 2010). *F. oxysporum* chromosomes can be categorised into two types: (1) 11 conserved chromosomes that are present in all strains; and (2) a variable number of 'accessory', or 'lineage-specific', chromosomes that can be acquired via HCT (Ma *et al.*, 2010). For HCT to occur, two germinating spores fuse, a haploid nucleus from each of the two strains fuse, and one strain's core chromosomes are systematically lost (Shahi *et al.*, 2016). In plant pathogenic strains of *F. oxysporum*, accessory chromosomes that are acquired via HCT may have the genes required for host-specific pathogenicity (i.e. a pathogenicity chromosome). However, while the process of HCT is understood, there are few documented examples of HCT in nature, and it is unknown how frequently HCT has contributed to the diversity of strains that cause disease on a particular host.

Many *formae speciales*, including *Fof* (Nagarajan *et al.*, 2006; Paynter *et al.*, 2016; Henry *et al.*, 2017), are polyphyletic and HCT provides an attractive explanation for this diversity. Where HCT occurred, virulence would be determined by the same genes, that is those residing on a shared pathogenicity chromosome (Ma *et al.*, 2010; van Dam *et al.*, 2017; Li *et al.*, 2020). However, given the vast genetic diversity observed in *F. oxysporum* (O'Donnell *et al.*, 2009), it is plausible that the same host specificity could be conferred by different repertoires of genes on nonhomologous pathogenicity chromosomes. These pathogenicity determinants could have accrued through independent processes of mutation (such as transposon activity, DNA copy error, etc.) and/or the acquisition of novel alleles through HCT. If true, polyphyly in a *forma specialis* could result from independently evolved genetic determinants of pathogenicity, not HCT alone.

Isolates with different genetic determinants of host specificity could also cause distinct disease phenotypes. Such phenotypic distinctions have been observed, for example *F. oxysporum* f. sp. *melonis* was differentiated into isolates that cause chlorosis ('yellows') or that only cause wilting ('wilts') (Jacobson & Gordon, 1988). It is not yet known if the 'yellows' and 'wilt' phenotypes of *F. oxysporum* f. sp. *melonis* resulted from independently evolved pathogenicity chromosomes. If so, the mechanisms responsible for inducing disease may differ, and genetic resistance may not function against both mechanisms.

Deployment of genetically resistant cultivars has been the most effective strategy for management of *Fusarium* wilt in many crops. All characterised host resistance (*R*) genes for *F. oxysporum* wilt pathogens function by recognising pathogen 'avirulence' proteins and subsequently initiating defence responses (Ori *et al.*, 1997; Joobeur *et al.*, 2004; Diener & Ausubel, 2005; Lv *et al.*, 2014; Catanzariti *et al.*, 2016). Mutations in pathogen avirulence genes can render the resulting protein imperceptible by the cognate host resistance protein. When these mutations occur, the pathogen is once again able to cause disease. This 'gene-for-gene' interaction is used to categorise pathogens into different 'races' based on the reaction of cultivars with different susceptibility phenotypes. Of the few, well documented avirulence genes in *F. oxysporum*, all are carried on pathogenicity chromosomes (Ma *et al.*, 2010; Catanzariti *et al.*, 2016; Schmidt *et al.*, 2016). Therefore, the efficacy of resistance genes may not extend to strains that do not share the same pathogenicity chromosome.

The objective of the present study was to characterise the evolutionary processes responsible for the emergence and diversification of the pathogen causing *Fusarium* wilt of strawberry. It has been unknown if the expanding geographic range of this pathogen resulted from dispersal of a clonal strain, whether horizontal transfer of a pathogenicity chromosome occurred, and/or if pathogenicity evolved independently on multiple continents. To identify the processes that resulted in the emergence of *Fof* we: (1) sampled isolates at a global scale, including historic isolates from the sites of first reports and more recent outbreaks; (2) investigated the evolutionary relationships between representative isolates from each country with comparative genomics/

transcriptomics; and (3) assessed the co-evolutionary framework of host and pathogen with comprehensive host resistance phenotyping. Here, we show that understanding the processes underlying pathogen diversification is important for the early identification of novel races and the development and deployment of genetic resistance to *Fusarium* wilt.

Materials and Methods

Isolate collection and initial characterisation

Corresponding authors from 15 publications reporting *Fof* in seven countries were contacted for the isolates used in their studies. Isolates were additionally obtained from the Queensland Herbarium culture collection (Australia) and the National Agricultural and Food Research Organisation Genebank (Japan). Isolate diversity was maximised by selecting representatives of the broadest variation in date of collection, region of origin, and genetically distinct groups (Supporting Information Dataset S1).

To reduce redundancy in subsequent experiments, we identified clonally related isolates by multilocus genotyping and a phenotypic test of clonality based on somatic compatibility. Isolates were determined to be compatible if complementary nitrate nonutilising mutants formed wild-type growth when co-cultured on a medium lacking reduced nitrogen (Correll *et al.*, 1987). Wild-type growth indicates that intra-isolate hyphal fusion occurred, allowing for complementation and effective utilisation of nitrate (Correll *et al.*, 1987). We sequenced the *translation elongation factor 1- α* (*EF-1 α*) and intergenic spacer (*IGS*) loci of all isolates as previously described by Henry *et al.* (2017). Isolates with the same two-locus haplotype that were somatically compatible were considered to be clonally related.

Pathogenicity assays with cultivars 'Sweet Ann' and 'Ventana'

To confirm the reported characterisation as *forma specialis fragariae*, we tested pathogenicity on strawberry for 31 putative *Fof* isolates that represented the observed spatiotemporal and genotypic diversity of clonal groups from each country. We additionally tested the pathogenicity of seven putative nonpathogenic *F. oxysporum* isolates from strawberry fields. Pathogenicity tests were conducted with cultivars that are known to be susceptible ('Sweet Ann') and resistant ('Ventana') to Californian strains of *Fof* (Pincot *et al.*, 2018). For each isolate, two fully colonised 100 cm potato dextrose agar (PDA) plates were blended with sterile, de-ionised water and mixed into #1 Sunshine mix (Sun Gro Horticulture, MA, USA) in a 10 × 10 × 20 cm pot (L × W × H). A single plant that had broken dormancy was then planted in each pot ($n=4$ per cultivar). Noninoculated PDA plates were used for a negative control. This experiment was conducted twice.

Plants were maintained in a growth chamber with 12 h : 12 h photoperiod, 28°C (high) : 20°C (low) temperature settings for 8 wk. Disease severity was assessed at 4, 5, 6, 7 and 8 wk post

inoculation (wpi) using a 1–5 ordinal rating system (Fig. S1). For isolates that did not cause chlorosis, ratings were based on the following symptoms: 1, no symptoms; 2, 0–25% of leaves wilted; 3, 25–50% of leaves wilted; 4, more than 50% of leaves wilted; and 5, dead (all leaves wilted/brown). For isolates that caused chlorosis, the rating scale was: 1, no symptoms; 2, mild stunting; marginal chlorosis; 3, youngest leaves fully chlorotic; 4, outer leaves chlorotic, some wilting observed; and 5, dead (all leaves were brown). At 8 wpi, or the time of plant mortality, four 2.5-cm sections from the base of petioles of each plant were surface sterilised with 1% sodium hypochlorite for 2 min and plated onto Komada's medium to confirm the recovery of the pathogen (Henry *et al.*, 2017).

Differences in symptom severity at 8 wpi on 'Sweet Ann' were compared between chlorosis-causing (yellows-*fragariae*), wilt-only causing (wilt-*fragariae*) isolates. The proportion of 'Sweet Ann' plants that were dead at 8 wpi was calculated for each isolate, with data pooled across both experiments ($n=8$). Plant mortality proportions were arcsin square root transformed to achieve a normal distribution (package: STATS, function: 'qqnorm'), and Welch's *t*-test was used to test the hypothesis that yellows-*fragariae* and wilt-*fragariae* isolate groups differed in mean mortality proportions at 8 wpi (package: STATS, function: *t.test*, R v.3.5.2) (R Core Team, 2013).

Whole genome sequencing and assembly

To investigate the evolutionary relationships between *Fof* isolates, we generated whole genome assemblies for representatives of all clonal groups of this pathogen present in each country (35 total), 12 nonpathogenic isolates from strawberry plants or field soil, and one isolate of *F. oxysporum* f. sp. *mori* (the cause of *Fusarium* wilt of blackberry; Dataset S1; Table S1). DNA was extracted from lyophilised mycelia or conidia using a phenol–chloroform extraction protocol (Kaur *et al.*, 2017). Libraries were prepared and sequenced on an Illumina NextSeq or HiSeq (150 bp, paired end) at the University of California, Davis DNA Technologies Core Facility or at the Michigan State University Genomics Core Facility. SMRTBell libraries were additionally prepared for GL1080 and GL1381, size selected to fragments greater than 15 kbp, and sequenced on a Pacific Biosciences (PacBio) RSII at the DNA Technologies Core Facility (Davis, CA). The ProxiMeta high-throughput chromatin conformation capture (Hi-C) library preparation kit (Phase Genomics; Seattle, WA) was used to prepare libraries from GL1381 and GL1080 germlings. Hi-C libraries were sequenced on an Illumina NovaSeq system with 150-bp paired-end reads.

Genomes were assembled for 48 isolates from 150-bp paired-end Illumina reads using *de novo* A5 assembler software (Tritt *et al.*, 2012). Chromosome-level assemblies were additionally generated for isolates GL1080 and GL1381. First, PacBio reads were assembled by the HGAP3 pipeline in SMRTANALYSIS (v.2.3.0) with default parameters (Chin *et al.*, 2013) and error corrected with PILON (v.1.23) from BOWTIE2-mapped Illumina reads (v.2.3.4.1; Langmead & Salzberg, 2012; Walker *et al.*, 2014). These assemblies were then scaffolded with Hi-C library

reads (113 and 49 million reads for GL1080 and GL1381) using the PROXIMO proprietary software from Phase Genomics, Inc. (Seattle, WA, USA). Scaffolded assemblies were gap-filled by PBJELLY (v.15.8.24) with proofread error-corrected PacBio reads (v.2.14.0; English *et al.*, 2012; Hackl *et al.*, 2014).

Core genome phylogenetic analysis

We analysed the core genome phylogenetic relationships between the 48 new assemblies and 91 previously published *F. oxysporum* genome assemblies ($n=139$ total). BUSCO (v.2.0) was run for every genome, and 2718 orthologues were identified as single copy in every genome (Simao *et al.*, 2015). Each of the 2718 genes were aligned with MUSCLE (v.3.8), and the alignments were concatenated (Edgar, 2004; Simao *et al.*, 2015). The maximum likelihood phylogeny of the concatenated alignment was determined by RAXML (v.8.2.12) using the general time reversible model with gamma correction and 1000 bootstrap replicates (Stamatakis, 2014). Phylograms were visualised by GGTREE (v.1.14.6; Yu *et al.*, 2017).

Gene and transposon annotation

The *in vitro* and *in planta* transcriptome of *F. oxysporum* f. sp. *lycopersici* 4287 has been sequenced previously (GenBank accession: GCA_000149955.2; van Dam *et al.*, 2016). We used HISAT2 (v.2.1.0) to align these reads to the reference genome (GenBank accession: GCA_000149955.2) with a maximum intron length of 6 kbp (Kim *et al.*, 2019). CUFFLINKS (v.2.2.1) was used to assemble and merge transcripts (Trapnell *et al.*, 2010). Assembled transcripts were used as evidence by CODINGQUARRY (v.2.0) to generate the gene models used during annotation (Testa *et al.*, 2015).

Using these pretrained gene models, we annotated all other genomes included in this analysis with CODINGQUARRY ($n=139$ genomes, in 'default' and 'pathogen mode'). Secreted proteins were predicted by SIGNALP4.1 (run mode = 'best') and EFFECTORP v.1.0 and v.2.0 were used for effector prediction (Nielsen, 2017; Sperschneider *et al.*, 2018). REPEATMODELER (v.1.0.11) and REPEATMASKER (v.4.0.8) were used to annotate transposable elements (Tarailo-Graovac & Chen, 2009). Miniature *impala* transposons were identified by TIRMITE (v.1.1.3) run four separate times with TIR alignments that collectively represent the breadth of miniature *impala* diversity (TIRMITE: <https://github.com/Adamtaranto/TIRmite>; 'mimp_finder.py' from REPERTOIRE v.6: https://github.com/pmhenry/Repertoire_v6).

Read mapping and coverage analysis

We identified conserved sequences in *Fof* by mapping reads to the GL1080 and GL1381 chromosome-level genomes. Raw reads were filtered with HTSTREAM to remove predicted PCR duplicates (hts_SUPERDEDUPER), remove Phi-X sequences (hts_SEQSCREENER), trim adapters (hts_ADAPTERTRIMMER), trim ends to an average quality value of '20' (hts_QWINDOWTRIM), and remove Ns from the ends of reads (hts_NTTRIMMER). To

ensure consistent read depth when mapping, 5.5 Gbp of quality-filtered reads were extracted for each isolate (*c.* 100× coverage; REFORMAT.SH from BBTools). These reads were aligned with BWA-MEM (v.0.7.17-r1188; Li & Durbin, 2009). BEDTOOLS (v.2.29.0) function ‘genomecov’ calculated the coverage of reads at each position in the genome, and regions with coverage greater than 9 were considered ‘present’ (Quinlan & Hall, 2010). To identify conserved sequences, coverage files were compared by BEDTOOLS ‘intersect -v’. To identify unique sequences, we used BEDTOOLS ‘subtract’.

Variant calling and SNP analysis

Because BUSCO genes were not evenly distributed among the chromosomes, we used variant calling to investigate the phylogeny of specific chromosomes and test for linkage disequilibrium. We called variants with FREEBAYES (v.1.3.1) using the following parameters: ‘--ploidy 1 --min-base-quality 20 --min-coverage 10 --min-alternate-fraction 0.4 --haplotype-length 0’ (Garrison & Marth, 2012). The output was filtered by VCFTOOLS to remove indels, require at least 70% of samples to have a genotype call, and exclude sites with minor allele count less than 2. The resulting SNPs were filtered by BEDTOOLS ‘intersect’ to remove SNPs that were not in regions with read coverage by all yellows-*fragariae* isolates. We used the VCFLIB function ‘vcfrandomsample’ to randomly extract SNPs from core chromosomes. Genotype calls were extracted into fasta formatted files by the ‘allele-seq’ function of VCFRIEND (<https://github.com/pmhenry/VCFriend>). Maximum likelihood phylogenetic analysis was conducted with RAXML (v.8.2.12) correcting for ascertainment bias with the following parameters: ‘-m ASC_GTRCAT -V --asc-corr = lewis’ (Stamatakis, 2014). Statistical support for each phylogeny was tested with 1000 bootstrap replicates.

For the index of association test of linkage disequilibrium, variants were called by FREEBAYES with a minimum minor allele frequency of 3 and no ‘--haplotype-length’ limit. For this analysis, we used a clone-corrected dataset that included 11 distinct genotypes of yellows-*fragariae*. Variants were randomly subsampled with the VCFLIB ‘vcfrandomsample’ to a rate of 0.05. The GL1080 chromosome-level assembly was used as the reference. Linkage disequilibrium was assessed by the R package POPPR function ‘ia()’ with 999 permutations (Kamvar *et al.*, 2015).

Transcriptomic experiments

To determine if genes on predicted pathogenicity chromosomes are differentially expressed during plant infection, we sequenced the *in vitro* and *in planta* transcriptome of a yellows-*fragariae* isolate. Tissue-cultured strawberry plants (cultivar ‘Camarosa’) were inoculated with a spore suspension of isolate GL1381 (*n* = 10 plants) as previously described, planted into twice-autoclaved sand and maintained in a growth chamber as previously described. Roots from five plants at each timepoint (6 d and 13 d post inoculation) were gently removed from sand, washed in sterile, de-ionised water and flash frozen in liquid nitrogen. For an *in vitro* control, GL1381 mycelia were scraped from PDA at 72 h

post inoculation and flash frozen in liquid nitrogen. RNA was extracted from these tissues with the 3% CTAB #1 protocol described in Yu *et al.* (2012). RNA was further purified by Ambion Turbo DNase treatment and the Zymo Research RNA Clean and Concentrate kit. RNA integrity was assessed with an Agilent Bioanalyser before 3′ QuantSeq library preparation (Lexogen, Inc.) with unique molecular indices. Libraries were sequenced on an Illumina NovaSeq (150 bp paired-end) to a minimum depth of 5 million reads per library.

Transcriptome quantification and analysis

Each read’s unique molecular index (UMI) was extracted with the ‘extract’ function from UMI tools (v.1.0.0; Smith *et al.*, 2017). Reads were filtered with HTStream and aligned with STAR (v.2.6.1a) to the GL1381 chromosome-level assembly (Dobin *et al.*, 2013). The aligned reads were deduplicated with UMI tools (Li *et al.*, 2009). Because the library preparation method selected primarily for sequences in 3′ un-translated regions (UTRs), we modified the count function in HTSEQ (v.0.6.1p1; Anders *et al.*, 2015) so that if a read aligned to overlapping UTR and CDS annotations from different genes, the transcript would be counted for the UTR-aligned gene. This program is available from: https://github.com/pmhenry/Publications/tree/master/Frag_Fof_TAGseq_Jenner_2020/HTSeq-TAG-Counts. Our modified ‘count’ function was used to generate read counts per gene from an annotation file where a 1000-bp UTR was added at the 3′ end of each gene. The program to add UTR annotations is available from: https://github.com/pmhenry/Publications/blob/master/Global_Fof_Henry_2020/TAGseq_gtf_annotation/tag_annotation.py.

Differential expression was evaluated in R using the EDGER package (Robinson *et al.*, 2010). Genes were filtered by FILTERBYEXPR, counts were transformed by VROOM, and linear models fit with LMFIT. *In planta* samples from 6 d and 13 d post inoculation were contrasted against *in vitro* samples. Genes with an adjusted *P*-value less than or equal to 0.05 and a log-fold change greater than 1.5 or less than −1.5 were considered to be differentially expressed.

Principal component analysis

In order to select diverse cultivars for resistance phenotyping, we analysed the genotypic diversity of available strawberry germplasm. These strawberry accessions had previously been genotyped on the Affymetrix® FanaSNP 50K Array (Hardigan *et al.*, 2020). Genotypes were called using the Affymetrix® Axiom Analysis Suite (v.4.0.1), and samples with a call-rate greater than 89% were retained for further analysis (Pincot *et al.*, 2018). The ‘A.mat’ function from the R package RRBLUP was used to construct a realised additive genetic relationship (A) matrix, filtering SNPs for a minor allele frequency of 0.05 and a maximum missing rate of 0.80 in the process (Endelman, 2011). Principal component analysis was run on the A matrix using the ‘prcomp’ command found in the base STATS package (R v.3.5.2; R Core Team, 2013).

Pathogenicity assays for cultivar differentials

We tested a panel of 25 diverse strawberry accessions against six strains of *Fof* that differed in their evolutionary origin or pathogenicity chromosome type. Conidia were harvested from isolates grown on PDA or Kerr's broth (Kerr, 1962). Bare-root transplants were submerged in 5×10^6 spores ml^{-1} of 0.1% water agar for 7 min before planting (Henry *et al.*, 2017). Pathogenicity assays with isolates MAFF727510, F79, BRIP62122 and AMP132 were conducted in a growth chamber with the settings indicated above. Strawberry accessions were also tested for resistance to isolate AMP132 in a field at the University of California, Davis Plant Pathology Farm (Methods S1). Isolates GL1315 and GL1381 were tested in a glasshouse in Salinas, California with 30°C (high) : 20°C (low) temperature settings. Each experiment was conducted at least twice, contained noninoculated controls, and two inoculated plants per accession \times isolate combination. A small number of accession \times isolate combinations had only one replicate in some experiments due to plant availability (Dataset S1). Least-squares means were generated using the LME4 (v.1.1-18-1) and EMMEANS packages (v.1.3.0; Bates *et al.*, 2015; Lenth, 2016; Lenth, 2018). Models were fit for each isolate with 'accession' as a fixed effect and 'experiment' and 'replication' as random effects.

Results

Isolate collection and characterisation

We obtained DNA or cultures of 85 *F. oxysporum* isolates from Australia, Japan, South Korea, Spain, and California (Dataset

S1). Twelve isolates did not cause symptoms on either cultivar. Of these, F74 and F79 were confirmed to be pathogenic on the cultivar Splendor, as previously reported (Borrero *et al.*, 2017). Isolate NRF0806 was still considered *Fof* based on reported pathogenicity to other cultivars (Suga *et al.*, 2013) and somatic compatibility with pathogenic isolates. Nine isolates did not meet these criteria and were therefore not considered to be *forma specialis fragariae*.

We considered any isolate that caused symptoms in both experiments to be pathogenic, and assumed (based on past research) that clones of pathogenic isolates were also pathogenic (Henry *et al.*, 2017). Given these criteria, we confirmed that 69 isolates were *Fof*. These isolates comprised 8 SCGs and 10 *EF-1 α /IGS* haplotypes (Dataset S1; Fig. S2; Table S1). One *EF-1 α /IGS* haplotype contained two SCGs (Fig. S2); 11 genotypes of *Fof* were therefore distinguished based on combined SCG and two-locus haplotypes.

Fof isolates cause two symptom phenotypes and can overcome FW1-mediated resistance

We observed two, distinct symptom phenotypes caused by *Fof*. Both phenotypic groups caused wilting and death. However, all isolates in two SCGs from Queensland in eastern Australia and an SCG from Spain caused little or no chlorosis (Fig. 1); we named these isolates 'wilt-*fragariae*' (Fig. 1a; Notes S1). All other pathogenic isolates, originating in Japan, South Korea, California and Western Australia caused severe chlorosis; we named these isolates 'yellows-*fragariae*' (Fig. 1a; Notes S1). Spanish wilt-*fragariae* isolates were pathogenic to 'Splendor', but not to 'Sweet Ann' or 'Ventana'. Results did not differ significantly between

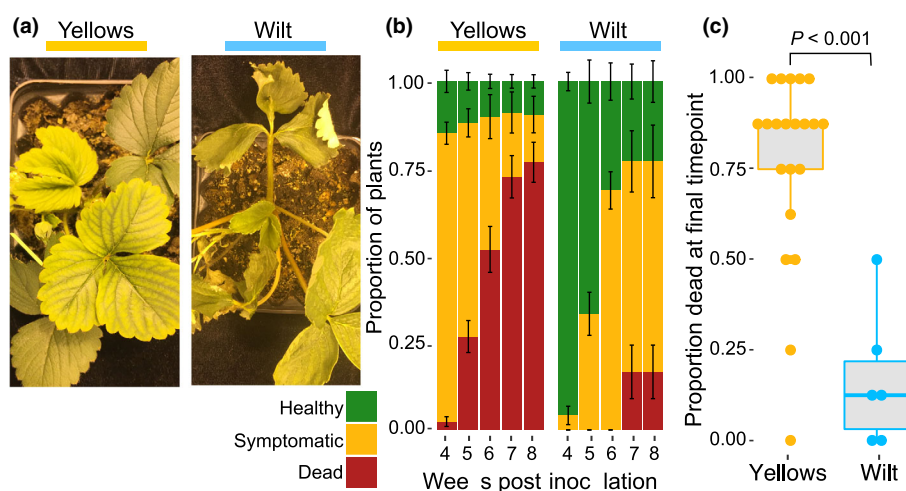


Fig. 1 Symptoms and disease severity induced by *Fusarium oxysporum* f. sp. *fragariae*. (a) The photograph on the left shows typical chlorosis symptoms caused by a yellows-*fragariae* isolate (N-18462) on new (inner) leaves observed 3 wk post inoculation. Symptoms caused by a wilt-*fragariae* isolate (BRIP62122) are shown on the right. (b) Disease severity at 4–8 wk post inoculation. The mean proportion of plants (cultivar 'Sweet Ann') that are healthy (green), symptomatic (yellow), or dead (red) for yellows- ($n = 21$) and wilt-*fragariae* ($n = 6$) isolates are reported. Proportions were calculated from the pooled results of two experiments in which four plants were inoculated per isolate ($n = 8$ plants total). The two experiments did not differ significantly in disease severity by a Kruskal–Wallis rank sum test ($df = 1$, $P = 0.1$). Error bars depict one standard error. (c) Boxplot depicting the proportion of 'Sweet Ann' plants that were dead by 8 wk post inoculation for each yellows- and wilt-*fragariae* isolate. Individual points correspond to each isolate in the yellows- and wilt-*fragariae* groups, for which there are 21 and 6, respectively. In each boxplot, the middle line corresponds to the median value, upper and lower bars correspond to first and third quartiles, respectively, and whiskers correspond to 1.5 times the interquartile range. The two symptom groups had significantly different proportions of dead plants per isolate at 8 wk post inoculation in a Kruskal–Wallis rank sum test ($df = 2$; $P < 0.001$).

experiments, so data were pooled in subsequent analyses ($P=0.1$, $df=1$ using Kruskal–Wallis rank sum test). Yellow-*fragariae* isolates caused greater disease severity than Australian wilt-*fragariae* on the susceptible cultivar Sweet Ann; the mortality of ‘Sweet Ann’ was higher at 8 wpi among plants inoculated with yellow-*fragariae* than with Australian wilt-*fragariae* (Welch’s t -test; $P<0.001$, $df=10$; Fig. 1b,c; R Core Team, 2013).

Five isolates consistently caused disease on the cultivar Ventana, which is heterozygous for the dominant *Fusarium* wilt resistance gene, *FW1* (Pincot *et al.*, 2018). *FW1*-resistance breaking isolates included four yellow-*fragariae* (MAFF727510, Fo160618, Fo160403 and SK1) and one wilt-*fragariae* isolate (BRIP62122). For each isolate, Wilcoxon rank sum tests showed no difference in virulence on the cultivars Ventana and Sweet Ann ($P\geq 0.24$). All isolates that caused disease on *FW1*-resistant cultivars were classified as ‘race 2’, whereas isolates that caused disease on ‘Sweet Ann’ but not ‘Ventana’ were classified as ‘race 1’. Spanish wilt-*fragariae* isolates did not receive a ‘race’ classification because they caused disease on ‘Splendor’ but not the other two cultivars, and the genetics of resistance to these isolates in ‘Sweet Ann’ is unknown.

Whole genome sequencing and assembly

Assemblies for all isolates generated from 150-bp paired-end reads had a high level of gene completeness; between 97.6% and 98.2% of BUSCO genes were present and single copy ($n=3725$ total searched; Dataset S1). For both of the GL1080 and GL1381 reference assemblies, >99% of the total genome length was assembled into 14 chromosome-sized scaffolds (Tables S2–S4; Fig. S3). In each assembly, 11 scaffolds corresponded to conserved chromosomes identified in the reference strain, *F. oxysporum* f. sp. *lycopersici* 4287 (Tables S2–S4; Fig. S3; Ma *et al.*, 2010). Each assembly additionally contained three accessory chromosomes that were not present in *F. oxysporum* f. sp. *lycopersici* 4287.

Fof is polyphyletic within *F. oxysporum* clade 2

To determine the core genome phylogeny of *Fof* isolates, we conducted maximum likelihood phylogenetic analysis on a 4.97 Mbp concatenated alignment of 2718 conserved, single copy orthologues (Stamatakis, 2014). Strong bootstrap support was observed for the three previously reported *F. oxysporum* clades (Figs 2, S4; O’Donnell *et al.*, 1998). We further resolved clade 2 into two subgroups (2A and 2B) with high bootstrap support (Figs 2, S4). Only Spanish wilt-*fragariae* isolates (called ‘W3’) were associated with clade 2A; all other wilt- and yellow-*fragariae* were in clade 2B (Figs 2, S4). Within clade 2B, yellow-*fragariae* isolates were in eight monophyletic clades (Y1–Y8) and Australian wilt-*fragariae* isolates were in two monophyletic clades (W1, W2; Figs 2, S4).

A putative mobile pathogenicity chromosome was identified in all yellow-*fragariae* isolates

We hypothesised that HCT occurred between yellow-*fragariae* strains because: (1) all isolates in this group caused the distinct

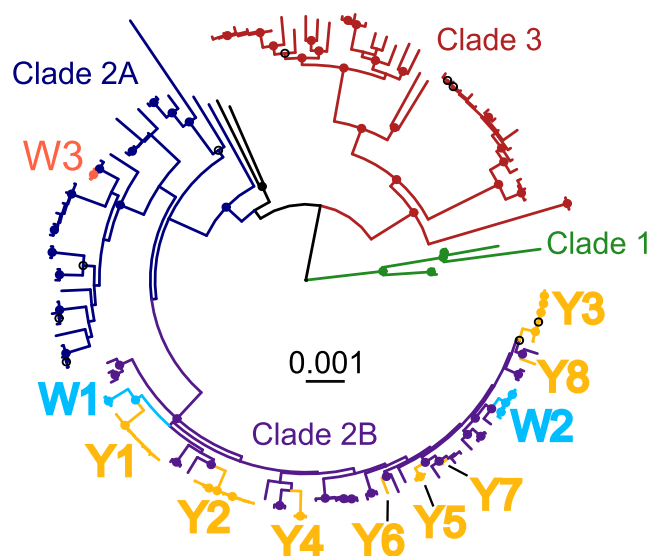
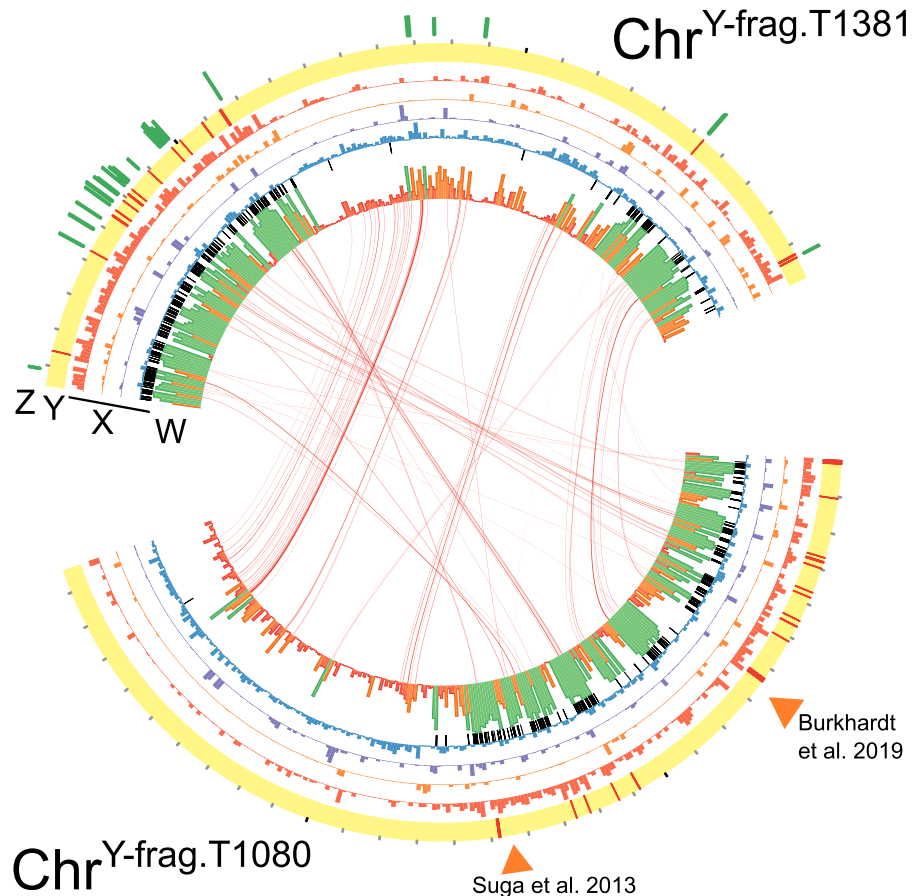


Fig. 2 Core genome phylogeny of the *Fusarium oxysporum* species complex with labels for monophyletic clades of *Fusarium oxysporum* f. sp. *fragariae*. Single copy orthologous genes ($n=2718$) from 139 *F. oxysporum* genomes were aligned by MUSCLE and concatenated into a single, c. 5.5 Mbp alignment. Maximum likelihood phylogenetic comparisons were conducted by RAxML using the general time reversible model with gamma correction and 1000 bootstrap replicates. Branches are colour-coded by *F. oxysporum* f. sp. *fragariae* symptom group (Spanish wilt-*fragariae* = W3, Australian wilt-*fragariae* = W1–W2, and yellow-*fragariae* = Y1–Y8) and by core genome phylogenetic clades. Nodes with a filled circle have bootstrap support >90%, a black open circle indicates bootstrap support >70%. Monophyletic groups of yellow- and wilt-*fragariae* are annotated as Y1–Y8 and W1–W3, respectively.

chlorosis phenotype; and (2) at least one isolate from each monophyletic group (Y1–Y8) possessed *forma specialis*-specific PCR-detection loci that were absent in wilt-*fragariae* isolates (Dataset S1; Suga *et al.*, 2013; Burkhardt *et al.*, 2019). To identify chromosomes that were putatively horizontally transferred, we mapped quality-filtered, 150-bp paired-end Illumina reads to the two reference genomes and identified one accessory contig in each genome that had large regions that were conserved among all yellow-*fragariae* isolates. These contigs also contained the yellow-*fragariae* PCR-detection loci and had the characteristics of previously discovered *F. oxysporum* mobile pathogenicity chromosomes: they were enriched with DNA transposons, carried most (58–65%) of the genome’s total miniature *impala* (*mimp*) transposons, and contained the only *secreted-in-xylem* (*SIX*) effector gene homologue (*SIX6*) (Figs 3, S3; Ma *et al.*, 2010; Schmidt *et al.*, 2013; van Dam *et al.*, 2017; Li *et al.*, 2020). Based on these results, they were hypothesised to be pathogenicity chromosomes: chr^{Y-frag.T1381} and chr^{Y-frag.T1080}.

chr^{Y-frag.T1080} and chr^{Y-frag.T1381} carried homologous sequences that were highly conserved among yellow-*fragariae* isolates. We identified 1.36 Mbp of chr^{Y-frag.T1381} and 1.29 Mbp of chr^{Y-frag.T1080} that were conserved in all yellow-*fragariae* isolates (Fig. 3; Datasets S2, S3). In these regions, there were 140 and 143 predicted genes in chr^{Y-frag.T1381} and chr^{Y-frag.T1080}, respectively. Based on reciprocal best BLAST hit matching, 82 of these genes were homologous (with sequence identity and coverage

Fig. 3 Synteny, sequence conservation, and differential expression of genes on chr^{Y-frag.T1381} and chr^{Y-frag.T1080}. (z) For GL1381, the log-fold change of *in planta* upregulated genes is shown by green bars on a scale from 0 to 15. (y) Red lines indicate the position of miniature *impala* transposable elements. Black tic marks occur every 100 kbp on the outside of the ideogram. (x) The proportion of each 10 kbp window covered by DNA transposons (red), LTR transposons (orange), LINEs (purple), or predicted genes (blue). Black lines indicate the position of sequences that are conserved in *yellow-fragariae* and are in no other *F. oxysporum* clade 2B isolate. (w) The proportion of each 10 kbp window with coverage in all *yellow-fragariae* isolates; green ≥ 0.66 , orange ≥ 0.34 , red < 0.33 . Links. Reciprocal best BLAST hits between predicted genes in the *yellow-fragariae* conserved regions of the two chromosomes are connected by red bands. Orange triangles indicate the positions of *yellow-fragariae*-specific detection loci identified by Suga *et al.* (2013) and Burkhardt *et al.* (2019).



thresholds of 0.8; Fig. 3). chr^{Y-frag.T1381} and chr^{Y-frag.T1080} contained 98.9% and 92.5% (respectively) of sequences that were conserved in *yellow-fragariae* and absent in all other clade 2B isolates (Fig. 3; Table S5). No other clade 2B isolate had complete coverage of the 1.36 Mbp of chr^{Y-frag.T1381} and 1.29 Mbp of chr^{Y-frag.T1080} that were conserved among *yellow-fragariae* isolates (Table S5). *Wilt-fragariae* isolates from eastern Australia shared at most 27% of conserved chr^{Y-frag} sequences, and this supports the hypothesis that wilt- and *yellow-fragariae* have different genetic determinants of pathogenicity (Table S5). These data indicated that, while not identical, chr^{Y-frag.T1080} and chr^{Y-frag.T1381} contained homologous sequences that are highly conserved within *yellow-fragariae*.

chr^{Y-frag} was horizontally transferred at least four times

The phylogeny of chr^{Y-frag.T1381} and chr^{Y-frag.T1080} provided compelling evidence for at least four HCT events. The phylogenies of chr^{Y-frag.T1381} and chr^{Y-frag.T1080} were nearly identical and distinct from the core chromosome phylogenies (Figs 4, S5). Branch lengths in the phylogenies of chr^{Y-frag.T1381} and chr^{Y-frag.T1080} indicated that at least six variants of this chromosome exist among *yellow-fragariae*, called: T1, T2, T3, T1381, T1080 and T1080B (Fig. 4). Phylogenetic incongruence provided evidence for a minimum of four HCT events: chr^{Y-frag.T1080} transferred between Y1 and Y6; chr^{Y-frag.T1381} transferred twice

between Y2, Y3 and Y4; and chr^{Y-frag.T1} transferred between Y2 and Y7 (Figs 4, S6).

These predicted HCT events were further supported by differences in read coverage of chr^{Y-frag.T1381} and chr^{Y-frag.T1080} by putative recipients. For example, GL1080 is in the Y1 group, but isolate Fo160609 (Y6) had 99% coverage of the 2.96 Mbp chr^{Y-frag.T1080} and 98.1% identical alleles at SNP sites (Figs S7, S8). Similarly, GL1381 is in the Y3 group, but >97% coverage and high sequence similarity of chr^{Y-frag.T1381} were observed for both Y4 isolates (NRF0833 and NRF0995; >98% identical) and two Y2 isolates (MAFF305557 and MAFF305558; >87.7% identical; Figs S7, S9). Two other Y2 isolates (GL1315 and GL1268) had >90% identical SNPs with a Y7 isolate (MAFF744009) and a nearly identical coverage pattern for chr^{Y-frag.T1381} and chr^{Y-frag.T1080}, suggesting that chr^{Y-frag.T1} was shared between these strains (Figs S7–S9). By contrast, other *yellow-fragariae* isolates had coverage for 70–86% of different chr^{Y-frag} types, and other clade 2B isolates had less than 75% coverage.

Although *F. oxysporum* is considered to be asexual, we looked for evidence of meiosis with an index of association test of linkage equilibrium. We conducted the index of association test on a clone-corrected dataset of *yellow-fragariae* isolates and discovered strong signatures of linkage disequilibrium on all chromosomes, including chr^{Y-frag} ($P=0.001$ for all chromosomes; Fig. S10). This indicates that meiosis is unlikely to explain the presence of chr^{Y-frag} in diverse *F. oxysporum* genotypes.

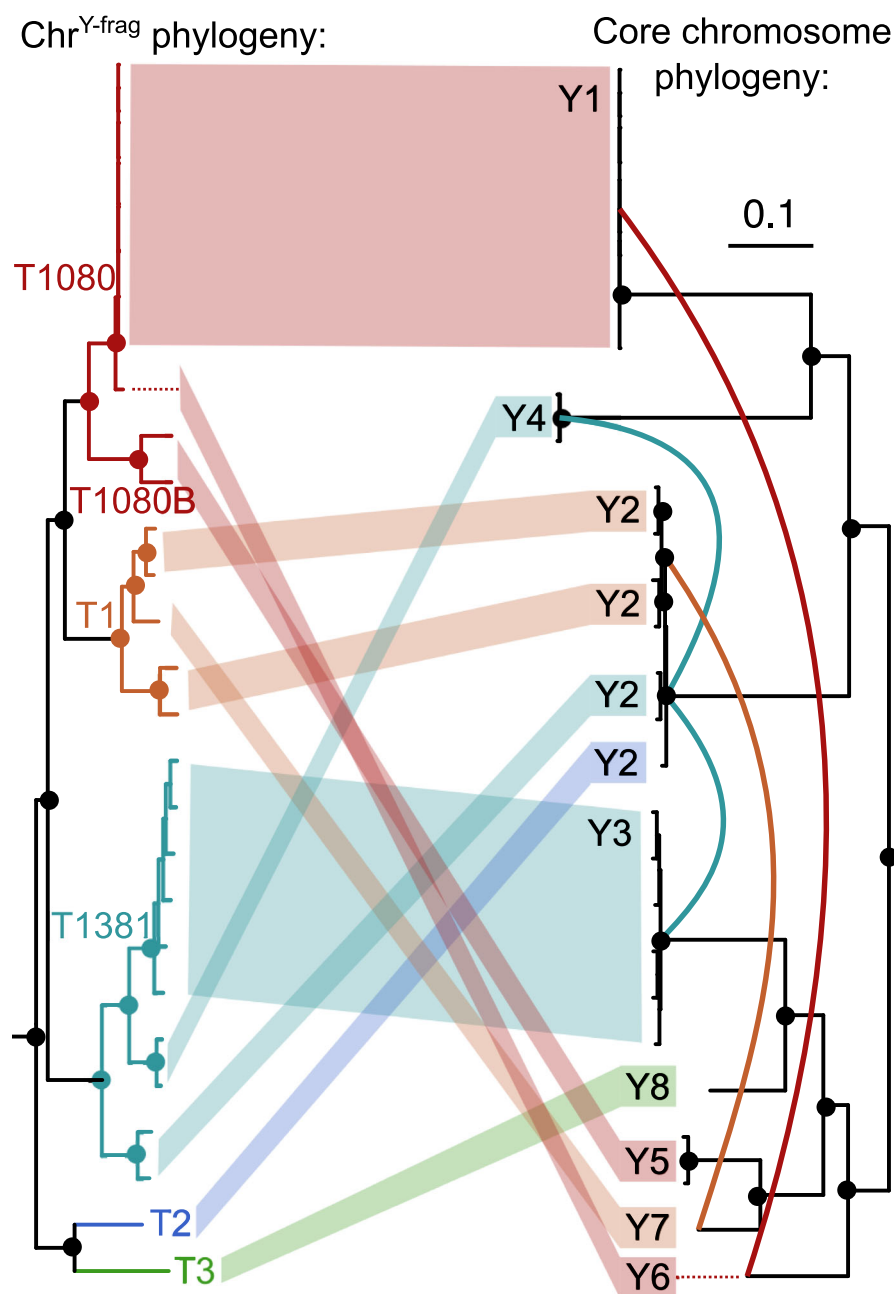


Fig. 4 Incongruence between the phylogeny of $\text{chr}^{\text{Y-frag.T1080}}$ and core chromosomes. Single nucleotide polymorphisms (SNPs) were called by FREEBAYES (v.1.3.1) on $\text{chr}^{\text{Y-frag.T1080}}$ and 11 core chromosomes from all 27 yellows-*fragariae* isolates. Genotype calls were concatenated for both datasets ($\text{chr}^{\text{Y-frag}}$ and combined core chromosomes), and the maximum likelihood phylogeny was inferred by RAXML with correction for ascertainment bias. Nodes with a filled circle have 100% bootstrap support. The $\text{chr}^{\text{Y-frag}}$ type (T1080, T1080B, T1381, T1, T2 and T3) is colour-coded and indicated adjacent to its corresponding clade. The monophyletic yellows-*fragariae* groups (Y1–Y8) are indicated next to their corresponding branches on the core genome phylogeny. Four predicted HCT events are indicated with solid, coloured lines between branches of the core genome phylogenetic tree.

$\text{chr}^{\text{Y-frag}}$ was probably polyphyletic before the first report of Fusarium wilt of strawberry

Phylogeny and sequence similarity suggested that $\text{chr}^{\text{Y-frag}}$ was present in multiple *F. oxysporum* genotypes before *Fusarium* wilt of strawberry was observed in Japan circa 1969 (Okamoto *et al.*, 1970). Within 20 yr of the first report, the isolates MAFF305557 (Y2), MAFF744009 (Y7) and MAFF727510 (Y8) were each recovered with distinct $\text{chr}^{\text{Y-frag}}$ types: T1381, T1 and T3, respectively (Fig. 4). If the level of divergence between $\text{chr}^{\text{Y-frag.T1381}}$ in Y3 and Y2 genotypes is typical for genetic drift over *c.* 20 yr (Figs 4, S7, S9), then all types of $\text{chr}^{\text{Y-frag}}$ could not have descended from a common ancestor after the observation of this pathogen in 1969.

$\text{chr}^{\text{Y-frag}}$ carries multiple effectors that are highly expressed during infection

GL1381's *in planta* transcriptome suggests that the expression of genes on $\text{chr}^{\text{Y-frag}}$ is associated with strawberry root infection. In total, 31 genes on $\text{chr}^{\text{Y-frag.T1381}}$ were differentially expressed *in planta* at 6 d or 13 d post inoculation compared with *in vitro* (adjusted *P*-value < 0.05, log-fold change > 1.5 or < −1.5) (Fig. 3; Dataset S1; Table S6). These genes were located in conserved regions among yellows-*fragariae* and were highly upregulated, with a 4.3–14.8 log-fold change in expression at 13 d post inoculation (Fig. 3; Dataset S1). Using EFFECTORP (v.1 and/or v.2), 12 of the 31 upregulated genes on $\text{chr}^{\text{Y-frag.T1381}}$ were predicted to be effectors, including a homologue of *SIX6* (Dataset S1;

Sperschneider *et al.*, 2018). Eight of these genes were present in all yellows-*fragariae* isolates. By contrast, only eight genes on lineage-specific chromosomes LS2 (2.70 Mbp) or LS3 (2.21 Mbp) were differentially expressed *in planta*, despite these chromosomes having a combined length (4.91 Mbp) that is almost double that of chr^{Y-frag.T1381} (2.75 Mbp) (Dataset S1; Fig. S3). No differentially expressed genes on LS2 or LS3 were conserved among all yellows-*fragariae* isolates (Dataset S1). The observed expression pattern supports the hypothesis that chr^{Y-frag.T1381} carries the genes necessary for host-specific pathogenicity.

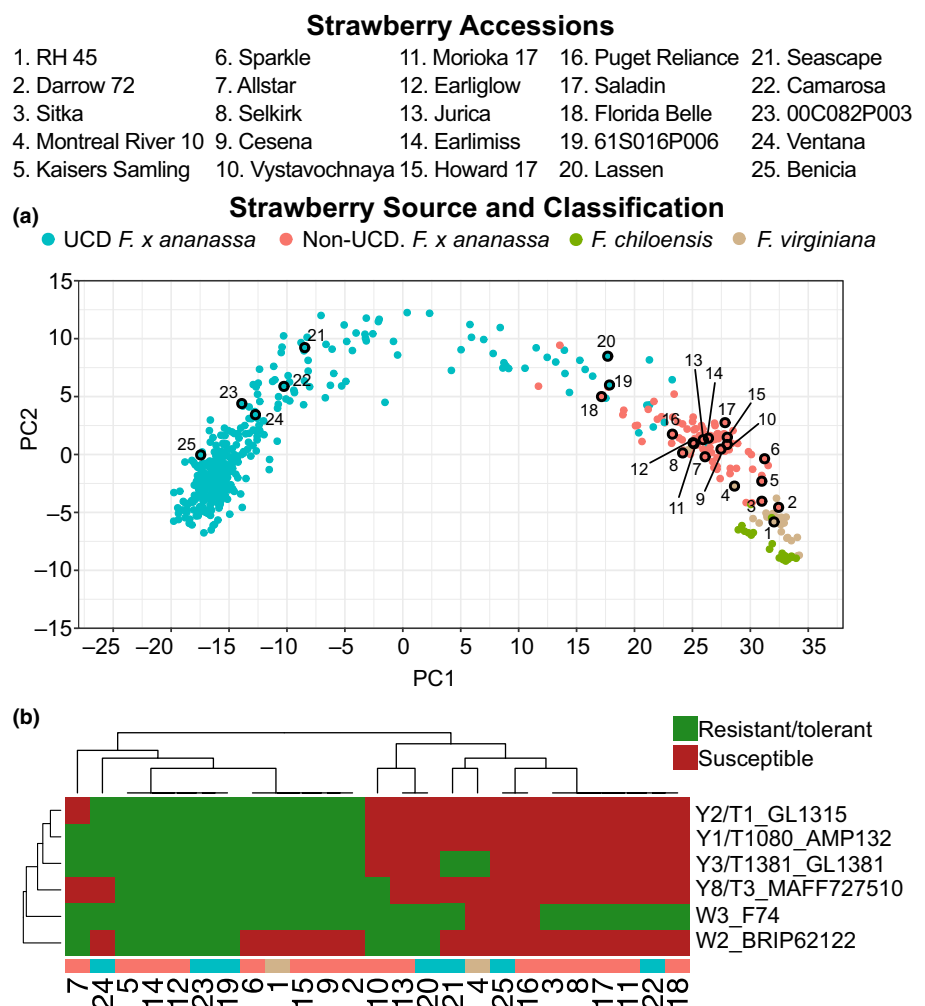
Differential host responses are associated with the presence of chr^{Y-frag}

Comparative genomics revealed that chr^{Y-frag} was only present in yellows-*fragariae* isolates; this chromosome was largely missing in strains of wilt-*fragariae* (Table S5). Given the transcriptomic results, we postulated that chr^{Y-frag} conferred common virulence/avirulence factors among the yellows-*fragariae* isolates. If true, host susceptibility would be more similar for yellows-*fragariae* isolates than between isolates of yellows- and wilt-*fragariae*.

Therefore, we hypothesised that isolates of yellows-*fragariae* from distinct monophyletic groups would have a similar cultivar host range, despite differences in core genome phylogeny. To test our hypothesis, we determined the phenotypic response of 25, diverse strawberry genotypes to four yellows-*fragariae* isolates (representing Y1/T1080, Y2/T1, Y3/T1381 and Y8/T3) and two wilt-*fragariae* isolates (representing W2 and W3). We used geographic, historic, and genotypic data (inferred from the octoploid Affymetrix® FanaSNP 50k array) to maximise diversity in the strawberry accessions tested (Hardigan *et al.*, 2020). Ultimately, we selected 23 *F. × ananassa* hybrids and two *F. virginiana* ecotypes (Fig. 5a; Datasets S1, S4).

Consistent with our hypothesis, we observed that the presence of chr^{Y-frag} is more predictive of cultivar susceptibility than core genome phylogeny. For example, the Y3 and Y8 core genomes are more closely related to W2 than Y1 and Y2 (Fig. 2) but have greater similarity in cultivar host range with the yellows-*fragariae* isolates (Figs 5b, S11). Between 80–96% of the strawberry accessions were consistently resistant or susceptible to yellows-*fragariae* isolates (Fig. S11). By contrast, only 52–68% of disease phenotypes were consistent between any yellows- and wilt-

Fig. 5 Genetic relatedness and resistance/susceptibility phenotypes of diverse strawberry accessions inoculated with *Fusarium oxysporum* f. sp. *fragariae*. (a) Principal component analysis (PCA) of 501 strawberry accessions estimated from the genotypes of 31 212 SNP markers assayed with the Affymetrix® FanaSNP 50K Array. The source and taxonomic classification of each accession is colour-coded; 'UCD' indicates cultivars developed at the University of California, Davis, and 'Non-UCD' indicates cultivars that were developed at other breeding programmes. Numbers correspond to the 25 cultivars phenotyped for resistance to six isolates of *F. oxysporum* f. sp. *fragariae*; their aliases are provided above the figure. (b) Disease phenotype of 25 strawberry accessions (columns) tested for resistance to six isolates of *F. oxysporum* f. sp. *fragariae* (rows). Disease severity was rated on a 1 to 5 ordinal scale, where 1 = symptomless and 5 = dead. Isolate cultivar combinations that had a least-squares mean disease severity score greater than or equal to 2.5 were considered 'susceptible' (red), and below 2.5 'resistant/tolerant' (green).



fragariae isolate (Figs 5b, S11). Therefore, cultivar host range is largely associated with the presence or absence of chr^{Y-frag}.

Discussion

Using isolates from multiple continents that were collected over time, including at the first reports of *Fusarium* wilt until present, we reconstruct the evolutionary and dispersal history of *Fof*. Of the two distinct syndromes we observed, yellows-*fragariae* isolates caused greater disease severity and were more widespread than wilt-*fragariae* isolates. Our data suggested that genes on chr^{Y-frag} conferred the pathogenicity phenotype to yellows-*fragariae* isolates, and horizontal transfer of chr^{Y-frag} has led to a polyphyletic distribution of this chromosome. The characterisation of chr^{Y-frag} as a mobile pathogenicity chromosome is supported by the conservation of chr^{Y-frag} among yellows-*fragariae*, *in planta* expression patterns, the association between its presence and host resistance/susceptibility phenotypes, and characteristic features that it shares with previously identified mobile pathogenicity chromosomes (Ma *et al.*, 2010; Schmidt *et al.*, 2013; van Dam *et al.*, 2017; Li *et al.*, 2020). We harnessed natural variation in the pathogen population to discover this chromosome; it was the only lineage-specific chromosome present in eight core genome phylogenetic groups of yellows-*fragariae*. chr^{Y-frag} was horizontally transferred at least four times, resulting in the diversification of this pathogen group. Experimental transfer of this chromosome *in vitro* and characterisation of recipients' pathogenicity phenotypes would provide an additional test of our hypothesis that HCT occurred among yellows-*fragariae* strains.

Pathogenicity in Australian and Spanish wilt-*fragariae* isolates appears to have evolved independently from yellows-*fragariae*, without chr^{Y-frag} (Notes S1, S2). This inference is primarily supported by: (1) sequences on chr^{Y-frag} that were conserved among yellows-*fragariae* were mostly absent in wilt-*fragariae* (Table S5); and (2) we discovered no evidence of sympatry between wilt- and yellows-*fragariae*, which would have been necessary for HCT to occur (Figs S11, S12). Furthermore, among isolates classified as wilt-*fragariae*, pathogenicity on strawberry appears to have evolved independently in both Spain and Australia. We observed no overlap in genotypic groups between these countries that could have provided evidence for dispersal. Both Spanish and Australian wilt-*fragariae* isolates are likely to possess other pathogenicity chromosomes that were not identified in the present study.

Other *formae speciales* have been classified into 'yellows' and 'wilt' syndromes (Edel-Hermann & Lecompte, 2019). To our knowledge, this is the first time that 'yellows' and 'wilt' syndromes have been shown to be caused by independently evolved pathogen genotypes that do not share a pathogenicity chromosome. Our results confirmed that disease phenotyping can facilitate the identification of evolutionarily distinct groups within a *forma specialis*.

Host resistance is a critical tool for disease management in many *Fusarium* wilt pathosystems, including *Fusarium* wilt of strawberry (Koike & Gordon, 2015). Here, we showed that isolates with a common pathogenicity chromosome have similar

cultivar host ranges, despite differences in core genome phylogeny. Therefore, differentiating between pathogen genotypes that emerged from transfer of a common pathogenicity chromosome versus a different pathogenicity chromosome has important implications for the identification and deployment of host resistance.

We observed a unique pattern of resistance/susceptibility for all six *Fof* genotypes we tested for pathogenicity on 25 diverse strawberry accessions (Fig. 5b). This result suggested that there were undiscovered gene-for-gene interactions that could ultimately demonstrate that each of these *Fof* genotypes is a different race. Here we propose race designations only when a differential interaction between the pathogen and a specific R-gene has been documented, following the commonly used convention (Bus *et al.*, 2011). In strawberry, only one *Fusarium* wilt resistance locus, *FW1*, has been identified (Pincot *et al.*, 2018). We report for the first time the existence of *Fof* 'race 2' isolates that overcome *FW1*-mediated resistance. The existence of this new race underscores the need to identify novel sources of resistance and breed them into commercially available cultivars.

Fortunately, our data suggested that numerous sources of resistance are available in hybrid cultivars and wild ecotypes. This is an unexpected finding, because we did not discover evidence of host-pathogen co-evolution. *Fragaria* × *ananassa* is an allo-octoploid ($2n = 8x = 56$) resulting from chance hybridisation between *F. chiloensis* (L. Miller) and *F. virginiana* (Duchesne), c. 300 yr before present (Darrow, 1966; Edger *et al.*, 2019). The native ranges of the wild octoploid progenitors span diverse biomes across North and South America (Staudt, 1988). The origins of *Fof* in Europe, Asia and Australia were separated by oceans from the natural range of these octoploid progenitors. This suggests that *Fof* did not co-evolve with its host and emerged from a host shift or host jump after the introduction of *F. × ananassa*. Therefore, *F. chiloensis* and *F. virginiana* should lack co-evolved defences that are specific to the *Fof* isolates we recovered. Consistent with this expectation, we found a wild *F. virginiana* ecotype that was susceptible to all pathogen genotypes (Fig. 5b). Why *F. chiloensis* and *F. virginiana* carry genes that confer resistance to a noncoevolved pathogen remains unclear. It is possible that genetic resistance evolved in response to genes in sympatric microorganisms that have homologues in *Fof*.

The selection pressures that led to the assembly of pathogenicity-enabling genes on chr^{Y-frag} remain unknown. Presumably, proto-pathogenicity chromosomes have been under selection for millennia in natural ecosystems. Given their role in plant infection, pathogenicity chromosomes could have initially evolved to facilitate asymptomatic, systemic colonisation of native plants (Gordon & Martyn, 1997). These strains could have emerged as pathogens through host shifts/jumps after the introduction of naïve agricultural crops, as has been postulated here for *Fof* and previously for *formae speciales vasinfectum* and *cubense* (Davis *et al.*, 1996; Ploetz & Pegg, 1997; Wang *et al.*, 2004).

Regardless of chr^{Y-frag}'s evolutionary origin, strains carrying this chromosome would have been amplified by widespread cultivation of strawberries. Our data suggested that this chromosome was present in multiple core genome backgrounds before the first

report of *Fusarium* wilt in Japan. However, commercial strawberry production began in Japan and South Korea in the early 20th century, long before the first observation of the disease in 1969 (Yoshida, 2013; Lee, 2014). If chr^{Y-frag} already existed in natural ecosystems, it could have taken several decades for strawberries to be planted in a field with a chr^{Y-frag}-carrying strain. Furthermore, initial inoculum densities were likely to be low, and many successive crops may have been required for disease to become apparent. Circumstances such as these could account for the delay between the introduction of strawberry agriculture and the first report of disease in 1969. Once abundant in strawberry production fields, isolates with chr^{Y-frag} were dispersed between Japan, South Korea, California and Western Australia, presumably on infected nursery plants (Notes S2; Fig. S6; Okamoto *et al.*, 1970; Nam *et al.*, 2011; Pastrana *et al.*, 2019). By contrast, we found no evidence that wilt-*fragariae* strains from eastern Australia or Spain have spread to other countries since their emergence.

We showed that HCT promoted diversification of *Fof*, but pathogenic genotypes also emerged independently, without receiving the same pathogenicity chromosome. These data supported the hypothesis that HCT is prevalent in *F. oxysporum* and has contributed to the evolution of many economically important plant pathogenic forms. The predicted pathogenicity chromosome chr^{Y-frag} is likely to have been present in multiple phylogenetic groups before *Fusarium* wilt of strawberry was observed in Japan. Knowledge of past HCT events informed an efficient approach to testing for host resistance; we found that the cultivar host range was more similar for isolates that shared a pathogenicity chromosome than for independently evolved pathogen genotypes. Geographic isolation suggests that all pathogenic lineages lack a history of co-evolution with *F. × ananassa* and its wild progenitors. However, we identified demographically and genetically diverse sources of resistance to this pathogen. Our results highlight the potential for comparative genomics of naturally diverse populations to reveal the evolutionary forces driving pathogen emergence and diversification.

Acknowledgements





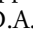
We thank Sam Koehler, Sukhwinder Kaur, Lia Lopez, Michelle Haugland, Mariel Munji, Samuel Brinker, Polly Goldman, and Shawn Melendy for providing technical assistance, and Dr Matthew Settles for providing general guidance on bioinformatics. Dr Haruhisa Suga, Michelle Paynter, Dean Beasley and Dr Youn-Sig Kwak are thanked for sending isolates of *F. oxysporum* f. sp. *fragariae*. We thank Joshua Puckett and the University of California, Davis Foundation Plant Services for providing tissue culture-derived strawberry plants for transcriptomics experiments. Thanks to our funding sources: the National Science Foundation Graduate Research Fellowship Program, the California Strawberry Commission, National Institute of Food and Agriculture (NIFA) Specialty Crops Research Initiative (#2017-51181-26833), pilot grants from the University of California, Davis, Bioinformatics and DNA Technologies Core Facilities, and Ministerio de Ciencia, Innovación y Universidades of Spain Project, Ref: RTI2018-094537-B-I00. The authors have no

conflicts of interest to declare regarding the research conducted or publication of this article.

Author Contributions

PMH, DDAP, SJK and TRG designed research; PMH, DDAP, BNJ, CB, MA and M-HN performed research; PMH, DDAP, LE analysed data; PMH wrote the paper; all authors read and revised the paper before submission.

ORCID

Celia Borrero  <https://orcid.org/0000-0002-6624-2518>
Lynn Epstein  <https://orcid.org/0000-0001-8697-1227>
Peter M. Henry  <https://orcid.org/0000-0002-7319-7516>
Steven J. Knapp  <https://orcid.org/0000-0001-6498-5409>
Dominique D.A. Pincot  <https://orcid.org/0000-0001-6463-1213>

Data availability

Information on isolates, genes of interest and disease phenotypes are included in Datasets S1–S4. GenBank accession codes and assembly statistics are listed in Dataset S1. All raw reads and assemblies for this project are available from BioProject accessions PRJNA578477 and PRJNA606324. Any additional data will be made available upon request.

References

- Anders S, Pyl PT, Huber W. 2015. HTSeq: a python framework to work with high-throughput sequencing data. *Bioinformatics* 31: 166–169.
- Bates DM, Mächler M, Bolker B, Walker S. 2015. Fitting linear mixed-effects models using *lme4*. *Journal of Statistical Software* 67: 1–48.
- Borrero C, Bascon J, Gallardo MA, Orta MS, Aviles M. 2017. New foci of strawberry *Fusarium* wilt in Huelva (Spain) and susceptibility of the most commonly used cultivars. *Scientia Horticulturae* 226: 85–90.
- Burkhardt A, Henry PM, Koike ST, Gordon TR, Martin F. 2019. Detection of *Fusarium oxysporum* f. sp. *fragariae* from infected strawberry plants. *Plant Disease* 103: 1006–1013.
- Bus VGM, Rikkerink EHA, Caffier V, Durel C-E, Plummer KM. 2011. Revision of the nomenclature of the differential host-pathogen interactions of *Venturia inaequalis* and *Malus*. *Annual Review of Phytopathology* 49: 391–413.
- Catanzariti A-M, Do HTT, Bru P, de Sain M, Thatcher LF, Rep M, Jones DA. 2016. The tomato *I* gene for *Fusarium* wilt resistance encodes an atypical leucine-rich repeat receptor-like protein whose function is nevertheless dependent on SOBIR1 and SERK3/BAK1. *The Plant Journal* 89: 1195–1209.
- Chin C-S, Alexander DH, Marks P, Klamm AA, Drake J, Heiner C, Clum A, Copeland A, Huddleston J, Eichler EE *et al.* 2013. Nonhybrid, finished microbial genome assemblies from long-read SMRT sequencing data. *Nature Methods* 10: 563–571.
- Correll JC, Klittich CJR, Leslie JF. 1987. Nitrate nonutilizing mutants of *Fusarium oxysporum* and their use in vegetative compatibility tests. *Phytopathology* 77: 1640–1646.
- van Dam P, Fokkens L, Ayukawa Y, van der Gragt M, ter Horst A, Brankovics B, Houterman PM, Arie T, Rep M. 2017. A mobile pathogenicity chromosome in *Fusarium oxysporum* for infection of multiple cucurbit species. *Scientific Reports* 7: 1–15.
- van Dam P, Fokkens L, Schmidt SM, Linmans JHJ, Kistler HC, Ma L, Rep M. 2016. Effector profiles distinguish formae speciales of *Fusarium oxysporum*. *Environmental Microbiology* 18: 4087–4102.

- Darrow GM. 1966. *The strawberry: history, breeding and physiology*. New York, NY, USA: Holt, Rinehart & Winston.
- Davis RD, Moore NY, Kochman JK. 1996. Characterisation of a population of *Fusarium oxysporum* f. sp. *vasinfectum* causing wilt of cotton in Australia. *Australian Journal of Agricultural Research* 47: 1143–1156.
- Diener AC, Ausubel FM. 2005. *RESISTANCE TO FUSARIUM OXYSPORUM 1*, a dominant *Arabidopsis* disease-resistance gene, is not race specific. *Genetics* 171: 305–321.
- Dobin A, Davis CA, Schlesinger F, Drenkow J, Zaleski C, Jha S, Batut P, Chaisson M, Gingeras TR. 2013. STAR: ultrafast universal RNA-seq aligner. *Bioinformatics* 29: 15–21.
- Edel-Hermann V, Lecompte C. 2019. Current status of *Fusarium oxysporum* formae speciales and races. *Phytopathology* 109: 512–530.
- Edgar R. 2004. MUSCLE: Multiple sequence alignment with high accuracy and high throughput. *Nucleic Acids Research* 32: 1792–1797.
- Edger PP, Poorten TJ, VanBuren R, Hardigan MA, Colle M, McKain MR, Smith RD, Teresi SJ, Nelson ADL, Wai CM *et al.* 2019. Origin and evolution of the octoploid strawberry genome. *Nature Genetics* 51: 541–547.
- Endelman JB. 2011. Ridge regression and other kernels for genomic selection with R package rrBLUP. *Plant Genome* 4: 250–255.
- English AC, Richards S, Han Y, Wang M, Vee V, Qu J, Qin X, Muzny DM, Reid JG, Worley KC *et al.* 2012. Mind the gap: upgrading genomes with Pacific Biosciences RS long-read sequencing technology. *PLoS ONE* 7: 1–12.
- Garrison E, Marth G. 2012. Haplotype-based variant detection from short-read sequencing. arXiv preprint 1207.3907v2: 1–9.
- Gordon TR, Martyn RD. 1997. The evolutionary biology of *Fusarium oxysporum*. *Annual Review of Phytopathology* 35: 111–128.
- Hackl T, Hedrich R, Schultz J, Förster F. 2014. *proovread*: large-scale high-accuracy PacBio correction through iterative short read consensus. *Bioinformatics* 30: 3004–3011.
- Hardigan MA, Feldmann MJ, Lorant A, Bird KA, Famula R, Acharya C, Cole GS, Edger PP, Knapp SJ. 2020. Genome synteny has been conserved among the octoploid progenitors of cultivated strawberry over millions of years of evolution. *Frontiers in Plant Science* 10: 1–17.
- Henry PM, Kirkpatrick SC, Islas CM, Pastrana AM, Yoshisato JA, Koike ST, Daugovich O, Gordon TR. 2017. The population of *Fusarium oxysporum* f. sp. *fragariae*, cause of Fusarium wilt of strawberry, in California. *Plant Disease* 101: 550–556.
- Jacobson DJ, Gordon TR. 1988. Vegetative compatibility and self-incompatibility within *Fusarium oxysporum* f. sp. *melonis*. *Phytopathology* 78: 668–672.
- Joobeur T, King J, Nolin SJ, Thomas CE, Dean RA. 2004. The Fusarium wilt resistance locus *Fom-2* of melon contains a single resistance gene with complex features. *The Plant Journal* 39: 283–297.
- Kamvar ZN, Brooks JC, Grünwald NJ. 2015. Novel R tools for analysis of genome-wide population genetic data with emphasis on clonality. *Frontiers in Genetics* 6: 208.
- Kaur S, Pham QA, Epstein L. 2017. High quality DNA from *Fusarium oxysporum* conidia suitable for library preparation and long read sequencing with PacBio. doi: 10.17504/protocols.io.i8ichue
- Kerr A. 1962. The root rot-*Fusarium* wilt complex of peas. *Australian Journal of Biological Sciences* 16: 55–69.
- Kim D, Paggi JM, Park C, Bennett C, Salzberg SL. 2019. Graph-based genome alignment and genotyping with HISAT2 and HISAT-genotype. *Nature Biotechnology* 37: 907–915.
- Kim CH, Seo HD, Cho WD, Kim SB. 1982. Studies on varietal resistance and chemical control to the wilt of strawberry caused by *Fusarium oxysporum*. *Korean Journal of Plant Protection* 21: 61–67.
- Koike ST, Gordon TR. 2015. Management of Fusarium wilt of strawberry. *Crop Protection* 73: 67–72.
- Langmead B, Salzberg SL. 2012. Fast gapped-read alignment with Bowtie 2. *Nature Methods* 9: 357–359.
- Lee WS. 2014. Production of ever-bearing strawberry and production technology in Korea. *Acta horticulturae* 1049: 561–564.
- Lenth R. 2016. Least-squares means: the R package lsmeans. *Journal of Statistical Software* 69: 1–33.
- Lenth R. 2018. *emmeans: Estimated marginal means, aka least-squares means*. [WWW document] URL <https://cran.r-project.org/web/packages/emmeans/index.html> [Accessed 1 September 2020].
- Li H, Durbin R. 2009. Fast and accurate short read alignment with Burrows-Wheeler transform. *Bioinformatics* 25: 1754–1760.
- Li H, Handsaker B, Wysoker A, Fennell T, Ruan J, Holmer N, Marth G, Abecasis G, Durbin R. 2009. The sequence alignment map format and SAMtools. *Bioinformatics* 25: 2078–2079.
- Li J, Fokkens L, van Dam P, Rep M. 2020. Related mobile pathogenicity chromosomes in *Fusarium oxysporum* determine host range on cucurbits. *Molecular Plant Pathology* 21: 761–776.
- Lv H, Fang Z, Yang L, Zhang Y, Wang Q, Liu Y, Zhuang M, Yang Y, Xie B, Liu B *et al.* 2014. Mapping and analysis of a novel candidate Fusarium wilt resistance gene *FOCI* in *Brassica oleracea*. *BMC Genomics* 15: 1–10.
- Ma L, van der Does HC, Borkovich KA, Coleman JJ, Daboussi M, Di Pietro A, Duffresne M, Freitag M, Grabherr M, Henrissat B *et al.* 2010. Comparative genomics reveals mobile pathogenicity chromosomes in *Fusarium*. *Nature* 464: 367–373.
- Nagarajan G, Kang SW, Nam MH, Song JY, Yoo SJ, Kim HG. 2006. Characterization of *Fusarium oxysporum* f. sp. *fragariae* based on vegetative compatibility group, random amplified polymorphic DNA and pathogenicity. *Plant Pathology Journal* 22: 222–229.
- Nam MH, Kang YJ, Lee IH, Kim HG, Chun C. 2011. Infection of daughter plants by *Fusarium oxysporum* f. sp. *fragariae* through runner propagation of strawberry. *Korean Journal of Horticultural Science and Technology* 29: 273–277.
- Nielsen H. 2017. Predicting secretory proteins with SignalP. In: Kihara D, ed. *Protein function prediction: methods in molecular biology*. New York, NY, USA: Humana Press, 59–73.
- O'Donnell K, Gueidan C, Sink S, Johnston PR, Crous PW, Glenn A, Riley R, Zitomer NC, Colyer P, Waalwijk C *et al.* 2009. A two-locus DNA sequence database for typing plant and human pathogens within the *Fusarium oxysporum* species complex. *Fungal Genetics and Biology* 46: 936–948.
- O'Donnell K, Kistler HC, Cigelnik E, Ploetz R. 1998. Multiple evolutionary origins of the fungus causing Panama disease of banana: Concordant evidence from nuclear and mitochondrial gene genealogies. *Proceedings of the National Academy of Sciences, USA* 95: 2044–2049.
- Okamoto H, Fujii S, Kato K, Yoshioka A. 1970. A new strawberry disease 'Fusarium wilt'. *Plant Protection* 24: 231–235.
- Ori N, Eshed Y, Paran I, Presting G, Aviv D, Tanksley S, Zamir D, Fluhr R. 1997. The *I2C* family from the wilt disease resistance locus *I2* belongs to the nucleotide binding, leucine-rich repeat superfamily of plant resistance genes. *The Plant Cell* 9: 521–532.
- Pastrana AM, Watson DC, Gordon TR. 2019. Transmission of *Fusarium oxysporum* f. sp. *fragariae* through stolons in strawberry plants. *Plant Disease* 103: 1249–1251.
- Paynter ML, Czişlowski E, Herrington ME, Aitken EAB. 2016. Differences in pathogenicity, genetic variability, and cultivar responses among isolates of *Fusarium oxysporum* from strawberry in Australia. *American Society of Horticultural Science* 141: 645–652.
- Pincot DDA, Poorten TJ, Hardigan MA, Harshman JM, Acharya CB, Cole GS, Gordon TR, Stueven M, Edger PP, Knapp S. 2018. Genome-wide association mapping uncovers *Fw1*, a dominant gene conferring resistance to Fusarium wilt in strawberry. *G3: Genes, Genomes, Genetics* 8: 1817–1828.
- Ploetz R, Pegg K. 1997. Fusarium wilt of banana and Wallace's line: Was the disease originally restricted to his Indo-Malayan region? *Australasian Plant Pathology* 26: 239–249.
- Quinlan AR, Hall IM. 2010. BEDTools: a flexible suite of utilities for comparing genomic features. *Bioinformatics* 26: 841–842.
- R Core Team. 2013. *R: A language and environment for statistical computing*. v.3.5.2. Vienna, Austria: R Foundation for Statistical Computing.
- Robinson MD, McCarthy DJ, Smyth GK. 2010. edgeR: A Bioconductor package for differential expression analysis of digital gene expression data. *Bioinformatics* 26: 139–140.
- Schmidt SM, Houterman PM, Schreiver I, Ma L, Amyotte S, Chellappan B, Boeren S, Takken FLW, Rep M. 2013. MITEs in the promoters of effector genes allow prediction of novel virulence genes in *Fusarium oxysporum*. *BMC Genomics* 14: 1–21.

- Schmidt SM, Lukaszewicz J, Farrer R, van Dam P, Bertoldo C, Rep M. 2016. Comparative genomics of *Fusarium oxysporum* f. sp. *melonis* reveals the secreted protein recognized by the *Fom-2* resistance gene in melon. *New Phytologist* 209: 307–318.
- Shahi S, Beerens B, Bosch M, Linmans JHJ, Rep M. 2016. Nuclear dynamics and genetic rearrangement in heterokaryotic colonies of *Fusarium oxysporum*. *Fungal Genetics and Biology* 91: 20–31.
- Simao FA, Waterhouse RM, Ioannidis P, Kriventseva EV, Zdobnov EM. 2015. BUSCO: assessing genome assembly and annotation completeness with single-copy orthologs. *Bioinformatics* 31: 3210–3212.
- Smith T, Heger A, Sudbery I. 2017. UMI-tools: Modeling sequencing errors in unique molecular identifiers to improve quantification accuracy. *Genome Research* 27: 491–499.
- Sperschneider J, Dodds PN, Gardiner DM, Singh KB, Taylor JM. 2018. Improved prediction of fungal effector proteins from secretomes with EffectorP 2.0. *Molecular Plant Pathology* 19: 2094–2110.
- Stamatakis A. 2014. RAxML version 8: a tool for phylogenetic analysis and post-analysis of large phylogenies. *Bioinformatics* 30: 1312–1313.
- Staudt G. 1988. The species of *Fragaria*, their taxonomy and geographical distribution. *Acta horticulturae* 265: 23–34.
- Suga H, Hirayama Y, Morishima M, Suzuki T, Kageyama K, Hyakumachi M. 2013. Development of PCR primers to identify *Fusarium oxysporum* f. sp. *fragariae*. *Plant Disease* 97: 619–625.
- Tarallo-Graovac M, Chen N. 2009. Using RepeatMasker to identify repetitive elements in genomic sequences. *Current Protocols in Bioinformatics* 4: 1–14.
- Taylor JW, Hann-Soden C, Branco S, Sylvain I, Ellison CE. 2015. Clonal reproduction in fungi. *Proceedings of the National Academy of Sciences, USA* 112: 8901–8908.
- Testa AC, Hane JK, Ellwood SR, Oliver RP. 2015. CodingQuarry: highly accurate hidden Markov model gene prediction in fungal genomes using RNA-seq transcripts. *BMC Genomics* 16: 1–12.
- Trapnell C, Williams B, Pertea G, Mortazavi A, Kwan G, van Baren J, Salzberg SL, Wold B, Pachter L. 2010. Transcript assembly and quantification by RNA-Seq reveals unannotated transcripts and isoform switching during cell differentiation. *Nature Biotechnology* 28: 511–515.
- Tritt A, Eisen JA, Facciotti MT, Darling AE. 2012. An integrated pipeline for de novo assembly of microbial genomes. *PLoS ONE* 7: 1–9.
- Walker BJ, Abeel T, Shea T, Priest M, Abouelliel A, Sakthikumar S, Cuomo CA, Zeng Q, Wortman J, Young SK *et al.* 2014. Pilon: An integrated tool for comprehensive microbial variant detection and genome assembly improvement. *PLoS ONE* 9: e112963.
- Wang B, Brubaker CL, Burdon JJ. 2004. *Fusarium* species and *Fusarium* wilt pathogens associated with native *Gossypium* populations in Australia. *Mycological Research* 108: 35–44.
- Winks BL, Williams YN. 1965. A wilt of strawberry caused by a new form of *Fusarium oxysporum*. *Queensland Journal of Agricultural and Animal Science* 22: 475–479.
- Yoshida Y. 2013. Strawberry production in Japan: History and progress in production technology and cultivar development. *International Journal of Fruit Science* 13: 103–113.
- Yu D, Tang H, Zhang Y, Yu H, Chen Q. 2012. Comparison and improvement of different methods of RNA isolation from strawberry. *Journal of Agricultural Science* 4: 51–56.
- Yu G, Smith D, Zhu H, Guan Y, Lam TT. 2017. ggtree: an R package for visualization and annotation of phylogenetic trees with their covariates and other associated data. *Methods in Ecology and Evolution* 8: 28–36.
- phenotypes at final timepoints (corresponding to Fig. 5), differentially expressed accessory genome genes in GL1381, and the metadata and least-squares means for all *Fragaria* spp. x isolate combinations tested in the differential resistance panel.
- Dataset S2** A ‘.bed’ formatted file with the coordinates of sequences in the GL1381 genome that are conserved among all 27 yellows-fragariae isolates tested.
- Dataset S3** A ‘.bed’ formatted file with the coordinates of sequences in the GL1080 genome that are conserved among all 27 yellows-fragariae isolates tested.
- Dataset S4** Genotype matrix for all *Fragaria* spp. analysed in this study.
- Fig. S1** Pictures corresponding to disease ratings for wilt- and yellows-*fragariae*.
- Fig. S2** Overview of two-locus phylogeny, somatic compatibility, and pathogenicity phenotypes on cv ‘Sweet Ann’ for isolates used in this study.
- Fig. S3** Whole genome comparison of coding sequences, transposon density and yellows-*fragariae* sequence conservation in GL1381 and GL1080 reference assemblies.
- Fig. S4** Core genome phylogeny of the *Fusarium oxysporum* species complex with isolate labels based on 2718 single copy orthologous genes.
- Fig. S5** Comparison of the phylogeny inferred from single nucleotide polymorphisms in yellows-*fragariae* conserved regions of chr^{Y-frag.T1080} and chr^{Y-frag.T1381}.
- Fig. S6** Predicted events of horizontal chromosome transfer (HCT) and dispersal of yellows-*fragariae* core and chr^{Y-frag} genotypes.
- Fig. S7** Distance matrices based on the proportion of identical genotypes at single nucleotide polymorphic sites (SNPs) on A) chr^{Y-frag.T1381} and B) chr^{Y-frag.T1080}.
- Fig. S8** Coverage of GL1080 accessory chromosomes (chr^{Y-frag.T1080}, lineage-specific #2 (LS2), and lineage-specific #3 (LS3)) by short, high-fidelity reads from yellows-*fragariae* isolates.
- Fig. S9** Coverage of GL1381 accessory chromosomes (chr^{Y-frag.T1381}, lineage-specific #2 (LS2), and lineage-specific #3 (LS3)) by short, high-fidelity reads from yellows-*fragariae* isolates.
- Fig. S10** Index of association tests of single nucleotide polymorphisms (SNPs) on core and accessory chromosomes from a clone-corrected yellows-*fragariae* population.

Supporting Information

Additional Supporting Information may be found online in the Supporting Information section at the end of the article.

Dataset S1 Isolate metadata, genome metadata, GenBank/SRA accessions, raw ordinal scores for *Fusarium* wilt resistance

Fig. S11 The proportion of identical disease phenotypes (resistant vs susceptible) between six isolates of *Fusarium oxysporum* f. sp. *fragariae*.

Fig. S12 World map of isolates characterised phenotypically and with whole genome sequencing for this study.

Methods S1 Detailed methods for experiments testing resistance to isolate AMP132 in a field near Davis, CA.

Notes S1 Additional notes on symptoms caused by yellows- and wilt-*fragariae*.

Notes S2 A partial reconstruction of the emergence, dispersal and diversification of *F. oxysporum* f. sp. *fragariae*.

Table S1 Summary of isolates characterised in this study.

Table S2 Assembly stats for scaffolded GL1080 and GL1381 genomes.

Table S3 Chromosome and unplaced scaffold lengths and stats for the GL1381 assembly.

Table S4 Chromosome and unplaced scaffold lengths and stats for the GL1080 assembly.

Table S5 The coverage of regions on chr^{Y-frag} that are conserved among yellows-*fragariae* isolates by *F. oxysporum* clade 2B isolates.

Table S6 Sequencing and mapping statistics for transcriptomic experiments with GL1381.

Please note: Wiley Blackwell are not responsible for the content or functionality of any Supporting Information supplied by the authors. Any queries (other than missing material) should be directed to the *New Phytologist* Central Office.



About New Phytologist

- *New Phytologist* is an electronic (online-only) journal owned by the New Phytologist Foundation, a **not-for-profit organization** dedicated to the promotion of plant science, facilitating projects from symposia to free access for our Tansley reviews and Tansley insights.
- Regular papers, Letters, Research reviews, Rapid reports and both Modelling/Theory and Methods papers are encouraged. We are committed to rapid processing, from online submission through to publication 'as ready' via *Early View* – our average time to decision is <26 days. There are **no page or colour charges** and a PDF version will be provided for each article.
- The journal is available online at Wiley Online Library. Visit **www.newphytologist.com** to search the articles and register for table of contents email alerts.
- If you have any questions, do get in touch with Central Office (np-centraloffice@lancaster.ac.uk) or, if it is more convenient, our USA Office (np-usaoffice@lancaster.ac.uk)
- For submission instructions, subscription and all the latest information visit **www.newphytologist.com**